Novel Scaling Parameter for Circulating Fluidized Beds

Ralf Kehlenbeck and John Yates
Dept. of Chemical Engineering, University College London, London WC1E 7JE, U.K.

Renzo Di Felice
Dipartimento di Ingegneria Chimica e di Processo, Università Degli Studi Di Genova, 16145 Genoa, Italy

Hermann Hofbauer and Reinhard Rauch
Technische Universität Wien, A-1060 Wien, Austria

Experimental results of a one-fifth scale cold laboratory model of a circulating fluidized-bed pilot plant for biomass gasification are reported here. Measurements revealed that the solid circulation rate is a function of the superficial gas velocity in the riser and the total mass load in the system. A novel dimensionless scaling parameter introduced describes the dimensionless mass turnover. Experiments were carried out varying both particle diameter, 170 $\mu m \le d \le 860$ μm, and density, 1,480 $kg/m^3 \le \rho_s \le 8{,}900$ kg/m^3. An excellent prediction for the mass turnover was obtained for mass loads varying from 1 to 15 kg and throughout the whole particle size and density range using the equations derived. Furthermore, the particle-size distribution is a scaling parameter to be matched between a model and an industrial plant.

Introduction

There is increasing interest in using biomass as a primary source of energy. It is currently contributing some 14% to the total world energy production, mainly in developing countries. Its use is expected to grow in the face of global warming since it is to all intents and purposes a carbon dioxide neutral energy source (*Nuclear Energy—The Future Climate,* 1999). The present work originated from a project aimed at designing a fluidized-bed pilot plant in which biomass is gasified with steam at about 800°C to produce a hydrogen-rich gas that powers a phosphoric acid fuel cell for the generation of electricity. The design calls for the residual char from the gasifier to be combusted in a riser blown with air, thereby providing the heat necessary to drive the endothermic gasification reaction. To aid the design and operation of the plant, it is necessary to have information on its hydrodynamic performance, and studies were carried out on a scaled model of the unit operated at ambient temperature and pressure.

Scaling is a procedure frequently used to characterize and study the design of large-scale units such as aircraft and industrial boilers. With specially developed scaling rules a small-scale laboratory model can be built that has similar hydrodynamic behavior to a large plant. Thus, initial experiments can be carried out on a low-cost laboratory rig in order to verify the operating conditions of an industrial unit. It is of great industrial interest to see how the data obtained on a laboratory scale can be related to a full-scale plant.

Several attempts to develop scaling parameters for fluidized beds have been reported (Horio et al., 1986; Zhang and Yang, 1987; Foscolo et al., 1990; Chan and Louge, 1992), but probably the best known and most widely used parameters are those derived by Glicksman et al. (extensively reported in Glicksman et al., 1994). On the basis of the governing equations of conservation of mass and momentum of fluid and particles, they derived a set of nondimensional parameters that must be matched in order to obtain hydrodynamic similarity between a model and a full-scale plant. Their so-called "full" set of scaling parameters is

$$\frac{\rho_f \rho_s d_p^3 g}{\mu^2}, \quad \frac{\rho_s}{\rho_f}, \quad \frac{u_0^2}{gD}, \quad \frac{\rho_f u_0 D}{\mu}, \quad \frac{G_s}{\rho_s u_0}, \quad \textit{bed geometry}, \quad \phi, \quad \text{PSD}. \tag{1}$$

Correspondence concerning this article should be addressed to J. Yates.

The dimensionless solid circulation rate is defined as

$$C_s = \frac{G_s}{\rho_s \cdot u_0}, \tag{2}$$

ϕ is the sphericity of the particles, and PSD their particle size distribution. By matching this set of parameters hydrodynamic similarity is almost obtained, as has been confirmed by several experimental investigations (Nicastro and Glicksman, 1984; Almstedt and Zakkay, 1990; Glicksman et al., 1991, 1993, 1994).

In the work to be described here, a one-fifth-scale cold model of a circulating fluidized-bed (CFB) pilot plant was built on the basis of the full set of scaling parameters given in Eq. 1. Using the cold model, the influence of the operating parameters on the hydrodynamics of the system was investigated, and in this article we present the results obtained for the solid circulation rate, C_s, that led to a novel scaling parameter for circulating fluidized beds. The next stage of the project will be to compare the results obtained with the cold model with data from the pilot plant.

Experimental Equipment

The basic design of the cold laboratory model is shown in Figure 1. The main parts were made out of Perspex in order to observe the fluid dynamics of the system visually.

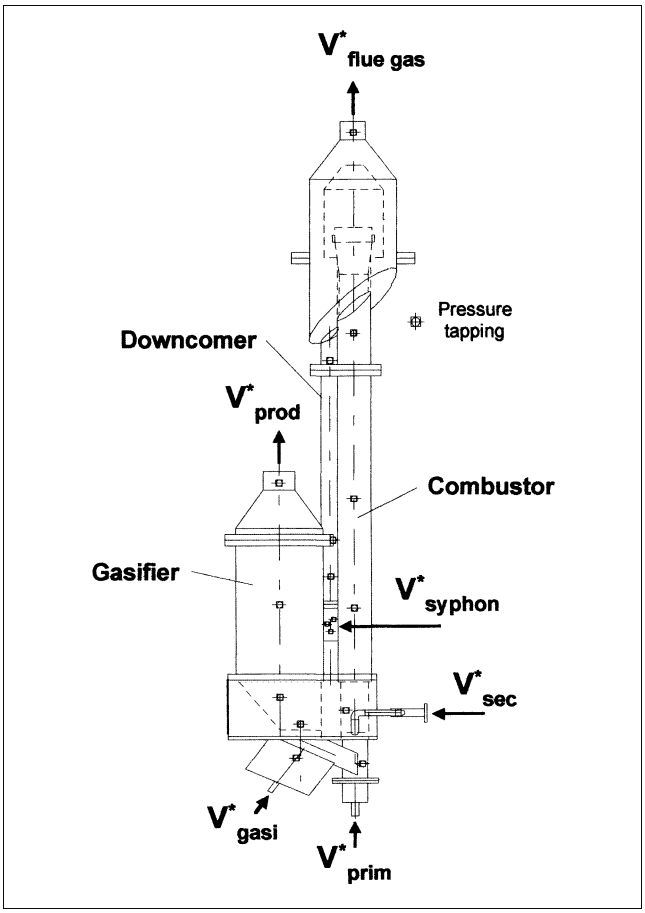

Figure 1. Basic design of the cold model.

The system can be divided into three main sections: a fluidized-bed gasifier ($D_{\text{gasi}} = 180$ mm), a riser–combustor ($D_{\text{comb}} = 54$ mm), and a downcomer ($D_{dc} = 24$ mm) that is separated from the gasifier by a siphon. The basic idea for the pilot plant is that the char resulting from the steam gasification of biomass is transported together with the circulating bed material (olivine) into the combustor (fluidized with air) where the char is partially burned. The exothermic combustion heats the olivine particles, which recirculate via the downcomer into the gasifier. The hot bed material provides the heat needed for the endothermic gasification. The volumetric flow rate into the windbox of the gasifier is indicated with V^*_{gasi}; the combustor has two air inlets, a primary, indicated with V^*_{prim}, and a secondary, indicated with V^*_{sec}. The flow rate into the primary inlet should be as low as possible in order to avoid gas crossflow into the gasifier, which would decrease the quality of the product gas by increasing its nitrogen content. Thus, with V^*_{prim} particles are lifted up to the secondary air inlet where the major air is injected. The ratio of $V^*_{\text{prim}}/V^*_{\text{sec}}$ is on the order of 15. In order to make the particles circulate from the downcomer into the gasifier, the syphon is fluidized with the flow rate V^*_{syphon}.

For the operation of the cold model, ambient air was chosen as fluidizing gas for the riser, and in order to match the required density ratio the gasifier was fluidized with a gas mixture of 55:45% helium to air. Spherical bronze particles with a measured density of 8,900 kg/m^3 and a mean particle diameter of 180 μm were chosen as bed material. Thus, the calculated scaling parameters for the pilot plant and the model were matched according to Glicksman et al. (1994).

Experimental Results

Solid concentration measurements

The distribution of solids volume fraction, c, in a CFB is of fundamental interest for many industrial applications since it influences, for example, the temperature distribution in the bed as well as any chemical reaction taking place; in a combustor good mixing between different components such as coke and ash is required.

Werther and Hirschberg (1997) divide the riser of a CFB into a dense bottom zone in which the hydrodynamics are similar to a bubbling fluidized bed, a transition zone, and an upper dilute zone that occupies most of the riser. In the dilute zone the solid volume fraction is on average of the order of 1%, and it can be divided again into two phases, namely, a lean core and a dense annulus in which the particle concentration is at least one order of magnitude higher than the solids volume fraction in the lean phase.

In order to calculate the voidage, $\epsilon = 1 - c$, in the riser of the model, the differential pressure drop between two successive pressure tappings (indicated in Figure 1) was measured. Thus, neglecting acceleration and friction forces, the voidage was calculated from

$$\epsilon = 1 - \frac{\Delta p'}{\Delta h} \cdot \frac{1}{(\rho_s - \rho) g}. \tag{3}$$

The voidage in the riser was measured for different solid mass loads in the system, and the results are shown in Figure 2 for total mass loads of 6 and 11 kg. It can be seen that ϵ

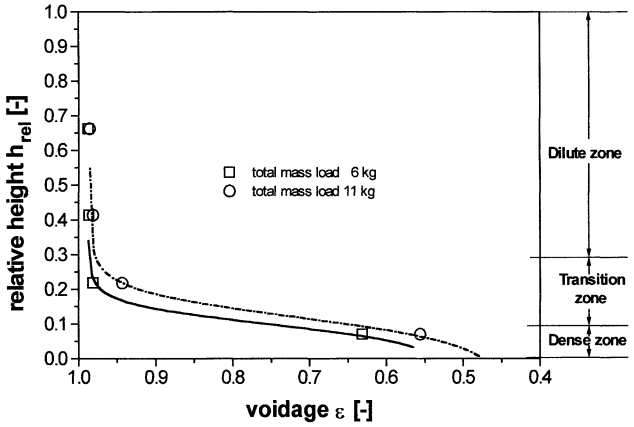

Figure 2. Voidage over the relative height of the riser.

for a mass load of 11 kg at a specific height in the riser is slightly lower than for a 6-kg mass load. The transition zone from the dense to the dilute phase is very narrow. Furthermore, at a riser height of about 20 to 30% the voidage is about 0.99 or, in other words, the solid concentration is about 1%, as just stated.

Solid circulation-rate measurements

The solid circulation rate is one of the basic operating parameters of a circulating fluidized bed, since it influences not only the temperature difference between the different sections of the reactor but also the residence times of particles, and therefore reaction and conversion times. For the gasification of biomass, for example, high temperatures are required in the gasifier for the tar pyrolysis (Spliethoff et al., 1996; Caballero et al., 1997), as well as for the efficiency of the catalyst to be used in the pilot plant to promote the production of hydrogen gas.

In the cold model the solid circulation rate could be determined by switching off the gas flow in the siphon of the downcomer, thereby preventing particles from flowing over into the gasifier; a fixed particle bed with a clearly defined surface then gradually filled the downcomer. Measuring the time, t, required for the particle bed to rise with respect to the bed height, h, the solid mass flow, m^*, was determined as

$$m^* = \frac{\pi}{4} D_{dc}^2 \frac{h}{t} \rho_s (1 - \epsilon_b), \tag{4}$$

and the mass flux, G_s, as

$$G_s = \frac{m^*}{A_{\text{comb}}} = \frac{D_{dc}^2}{D_{\text{comb}}^2} \frac{h}{t} \rho_s (1 - \epsilon_b), \tag{5}$$

where D_{dc} is the diameter of the downcomer and D_{comb} is the diameter of the riser (combustor). In addition to bronze, sand, salt, and Amberlite resin particles were studied. The measured particle properties are listed in Table 1.

Three parameters of possible influence on the circulation rate were investigated:

1. Volumetric flow rate into the gasifier, V_{gasi}^*
2. Volumetric flow rate into the riser, V_{prim}^* and V_{sec}^*
3. Total mass load in the unit, m.

Table 1. Measured Particles Properties for All Particles Used

	Bronze	Sand	Salt	Amberlite Resin
d_s (μm)	180	170	348	230/860
ρ_s (kg/m^3)	8,900	2,622	2,150	1,480
ϵ_b	0.4	0.44	0.42	0.40/0.44
u_t (m/s)	3.4	1.4	2.3	1.2/4.37

In Figure 3 the solid mass flux, G_s, is shown as a function of the volumetric flow rate into the gasifier, while both the flow rate in the primary and the secondary gas inlet of the combustor, V_{prim}^* and V_{sec}^*, as well as the mass load in the bed, were kept constant. It is evident the the solid circulation does not depend on V_{gasi}^*. Furthermore, no difference in circulation rate was observed by using air only as a fluidizing gas in the gasifier as an alternative to the gas mixture of helium-air required for the scaling.

In a second series of investigations the respective flow rates in the combustor section were varied as was the total mass load in the rig. The results obtained for G_s are shown in Figure 4 as a function of the superficial velocity, u_0, in the riser; no difference in circulation rate was observed by varying both the primary and secondary flow rate into the combustor as long as the total superficial velocity, u_0, calculated as

$$u_0 = \frac{V_{\text{prim}}^* + V_{\text{sec}}^*}{\pi/4 \cdot D_{\text{comb}}^2}, \tag{6}$$

was kept constant.

Horio (1997) has stated that in a CFB combustor the solid flux should be on the order of 10 to 30 kg/m^2·s, and it is evident from Figure 4 that this value is reached easily with the model investigated here. Furthermore, it can be seen that the solid mass flux increases strongly with increasing superficial velocity over the range investigated, and it is clear that at

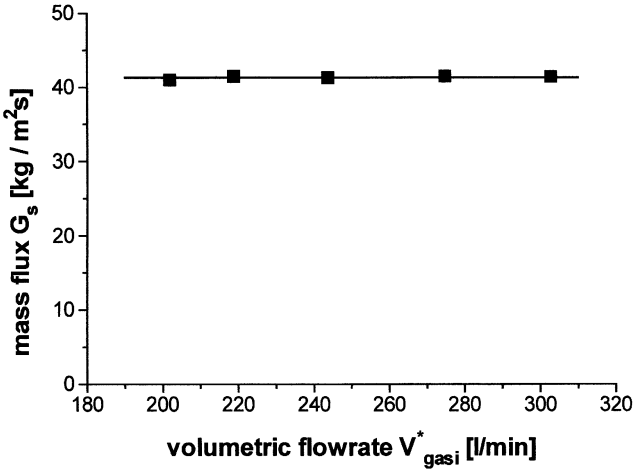

Figure 3. Solid mass flux as a function of the gas flow rate in the gasifier.

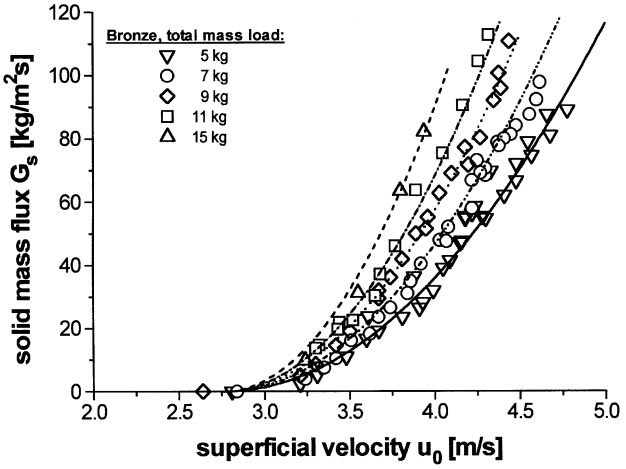

Figure 4. Solid mass flux as a function of the superficial gas velocity in the riser.

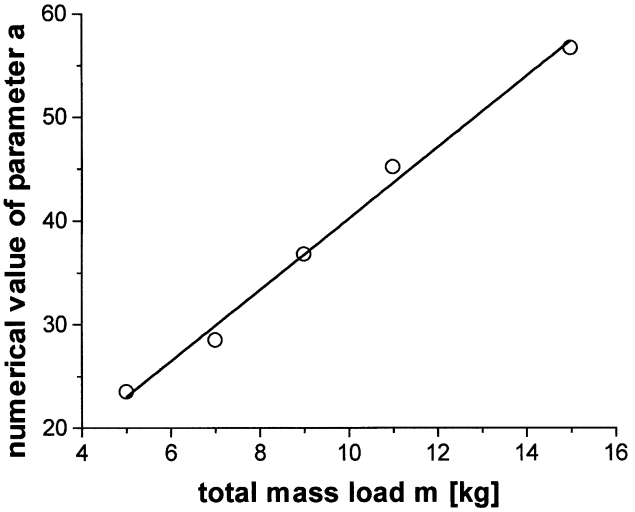

Figure 5. Dependency of the numerical value of the parameter *a* on the total mass load *m*.

a given value of u_0, G_s increases with increasing total mass load in the reactor.

The experimental data for the numerical value of the solid mass flux can be approximated as a function of the superficial velocity with a second-order function:

$$G_s = au_0^2 + bu_0 + c, \tag{7}$$

with the fitting parameters a, b, and c. Taking into account that solid circulation starts for the same fluid–particle system at a constant superficial velocity, $u_{0,\,\mathrm{start}}$, Eq. 7 can be reduced to a function, depending only on one fitting parameter applying the boundary condition:

$$G_s(u_0 = 2.75) = 0. \tag{8}$$

Equation 7 thus results in

$$G_s = au_0^2 - 5.5\ au_0 + 7.56\ a. \tag{9}$$

In Figure 5 the numerical value of the parameter a is shown as a function of the total mass load in the reactor and it is clear that a linear dependency is obtained, which can be expressed by

$$a = 3.43\ m + 5.85. \tag{10}$$

Although the preceding equations fit the data very well, they are dimensionally inconsistent, and so an approach was adopted based on dimensionless groups in order to fit the measured solid circulation rates. Hence the dimensionless group, C_s, proposed by Glicksman et al. (1994), was plotted for the bronze particles in Figure 6 as a function of a dimensionless velocity, U, defined as:

$$U = \frac{u_0}{u_t}, \tag{11}$$

where u_t represents the terminal settling velocity of a single particle calculated by

$$u_t = \sqrt{\frac{4}{3}\left(\frac{\rho_s - \rho}{\rho}\right)\frac{dg}{c_D}}\ . \tag{12}$$

The drag coefficient, c_D, was calculated as (Molerus, 1993)

$$c_D = \frac{24}{Re} + \frac{4}{\sqrt{Re}} + 0.4. \tag{13}$$

As discussed earlier, the solid volume fraction in the upper dilute zone of the riser of the CFB is less than about 1%, and it can be assumed that the forces acting between particles are negligible. A balance of forces acting on a single particle will

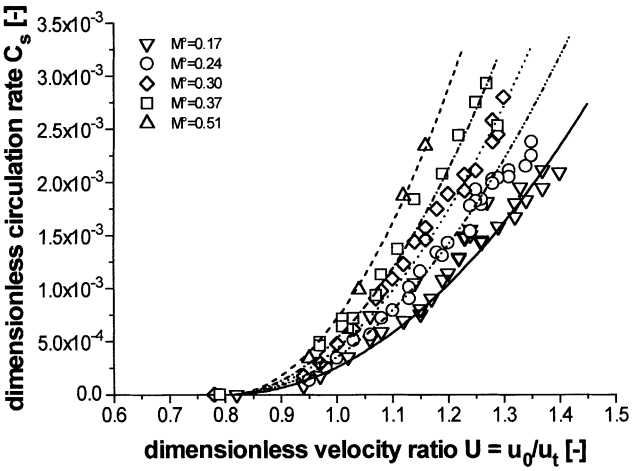

Figure 6. Dimensionless solid circulation rate of bronze particles as a function of the dimensionless gas velocity *U*.

correspond to a balance of the two velocities u_0 and u_t, and consequently u_t was chosen to make u_0 dimensionless rather than u_{mf}, as suggested by Glicksman et al. (1993). This means that for a given value of U, particles are lifted over a certain height in the riser, and for a given system geometry, solid circulation starts at one constant value of U for any fluid–particle system.

The total mass load in the bed, m, was nondimensionalized by dividing it by the total possible mass in the riser:

$$M^\circ = \frac{m}{V_{\text{comb}}\,\rho_s}. \tag{14}$$

From Figure 6 it is clear that, as is to be expected, solid circulation starts at a value of the superficial gas velocity close to u_t.

The experimental data shown in Figure 6 were fitted with an equation of the same form as Eq. 7, but are now based on dimensionless parameters:

$$C_s = a^*\,U^2 + b^*\,U + c^*. \tag{15}$$

With the boundary condition

$$\left.\frac{dC_s}{dU}\right|_{U_{\text{start}}=0.8} = 0, \tag{16}$$

Eq. 17 results in

$$C_s = a^*\,U^2 - 1.6a^*\,U + 0.64\,a^* \tag{17}$$

In Figure 7 the value of a^* is shown as a function of the dimensionless mass load, M°, in the reactor. Also here a linear dependency is obtained that can be expressed by

$$a^* = 0.03359\,M^o + 0.00076. \tag{18}$$

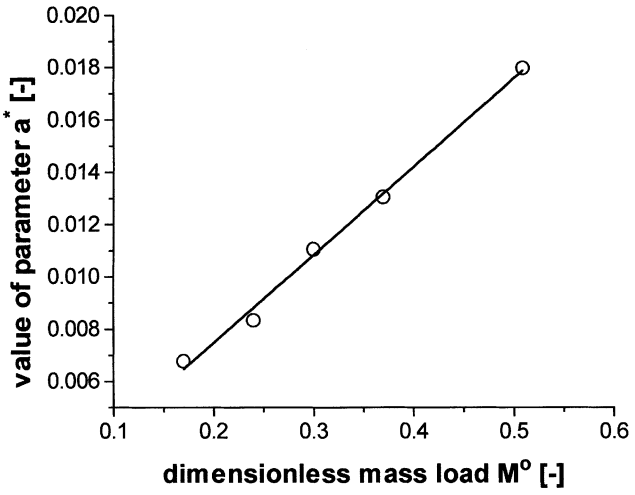

Figure 7. Value of the fitting parameter a^* as a function of the dimensionless mass load M°.

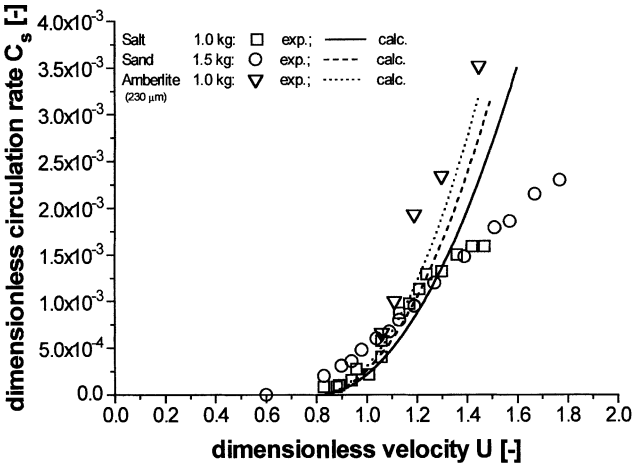

Figure 8. Dimensionless solid circulation rate as a function of the dimensionless gas velocity U.

In a further experiment the general validity of the proposed equations was tested. Figure 8 shows the results obtained for the different bed materials—salt, sand, and Amberlite resin (different particle sizes); the particle properties are listed in Table 1. The experimental values of C_s as a function of U are compared to the calculated values obtained with Eqs. 17 and 18. It is clear that for these particles the accuracy of the model over the range investigated is not very good, although the trend of the curves is predicted quite well. The assumption made before, however, that solid circulation starts at one specific value of velocity ratio, U, for any type of particle load but one specific apparatus, is confirmed here.

Novel correlation for the solid circulation rate

From the evidence presented in Figures 6 and 8, it was concluded that C_s is not a parameter that allows the prediction of a solid circulation rate as a function of the total mass load in the system, nor for different bed materials, and as a consequence an alternative defining parameter was sought based on the mass loadings investigated.

Figure 9 shows the solid mass flux, G_s, obtained for bronze particles as a function of m for a similar superficial velocity in the riser, and it can be seen that the relationship is linear. On the basis of this relationship, a novel parameter, the dimensionless mass turnover, M, was defined as follows:

$$M = \frac{m^*}{m}\cdot\frac{D_{\text{comb}}}{u_t}. \tag{19}$$

Plotting this dimensionless group against the dimensionless velocity, U, all data points obtained for bronze at different mass loadings fall onto one curve, as expected. These data are shown in Figure 10 together with the data obtained for sand, salt, and the resin, and it can be seen that apart from the beds of salt and sand, the data points all lie on one curve and that solid circulation starts for each bed material at the same value of U. The deviations shown by the experiments with salt and sand are thought to be due to the fact that both materials had a wider size distribution than that of the other

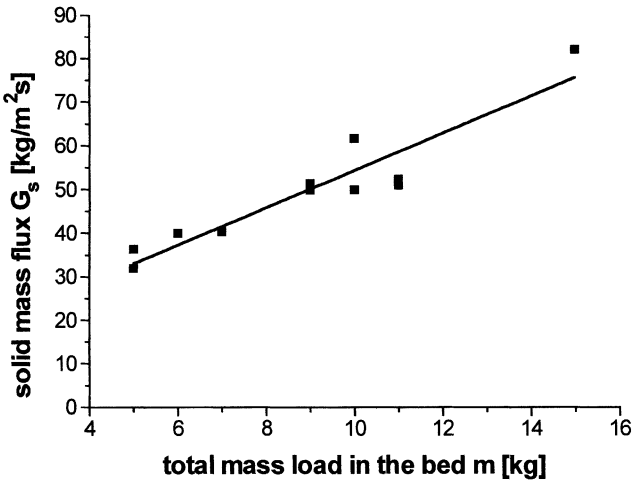

Figure 9. Solid mass flux as a function of the total mass load in the bed.

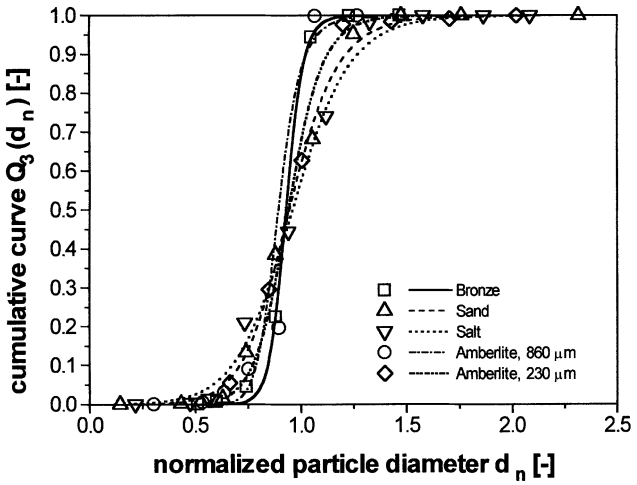

Figure 11. Normalized size distribution of the particles used.

solids investigated; this question is discussed in more detail below.

The dimensionless mass turnover can be correlated with a similar equation to the one derived earlier for G_s and C_s

$$M = a^o\, U^2 - 1.6a^o\, U + 0.64\, a^o, \tag{20}$$

with

$$a^o = 0.0015. \tag{21}$$

Equations 20 and 21 are plotted as a continuous line in Figure 10, and it can be seen that all the data are approximated with a very simple equation, depending on the one parameter a°.

Examination of Figure 10 shows that for sand at low-velocity ratios, U, the mass turnover is underpredicted, while for higher U the mass turnover is overpredicted. It is assumed that this resulted from differences in particle-size distribution (PSD). The normalized PSD of the particles used are compared in Figure 11, from which it is clear that, compared to the size distribution of bronze, sand has a higher fraction of both small and large particles.

Additional experiments were carried out using sand of different size distributions (shown in Figure 12). Case 1 represents the sand used previously, and case 2 refers to sand with an even higher fraction of the larger particles.

Solid circulation rates for these two materials were measured, and the results obtained are shown in Figure 13, from which it can be seen that for sand 2 the circulation rate is less than for sand 1 as a result of its higher proportion of large particles.

The sand used in the earlier experiments had a wider PSD than the bronze particles, that is, it contained a higher portion of both small and large particles, and thus it is to be expected that the solid circulation will start at lower values of U and that the slope of the curve with increasing U will be less than that for bronze. A similar argument applies to the salt particles.

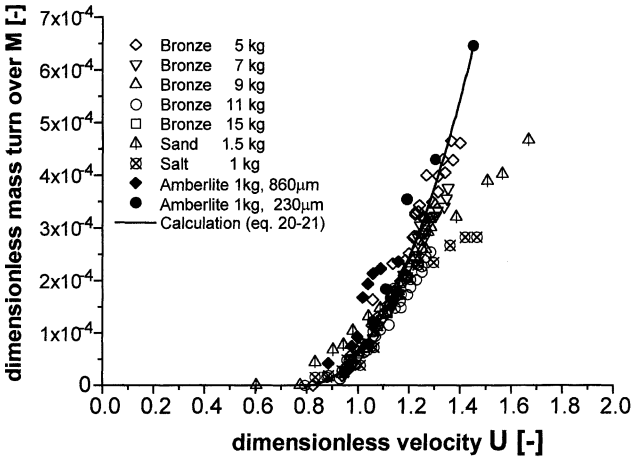

Figure 10. Dimensionless mass turnover *M* as a function of the dimensionless gas velocity *U*.

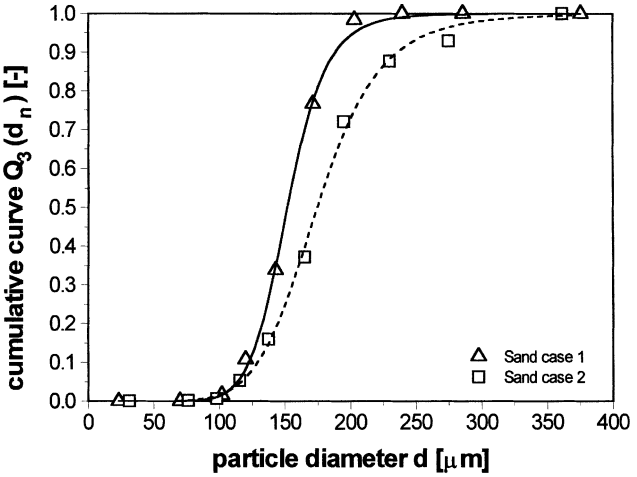

Figure 12. Size distribution of sand particles used.

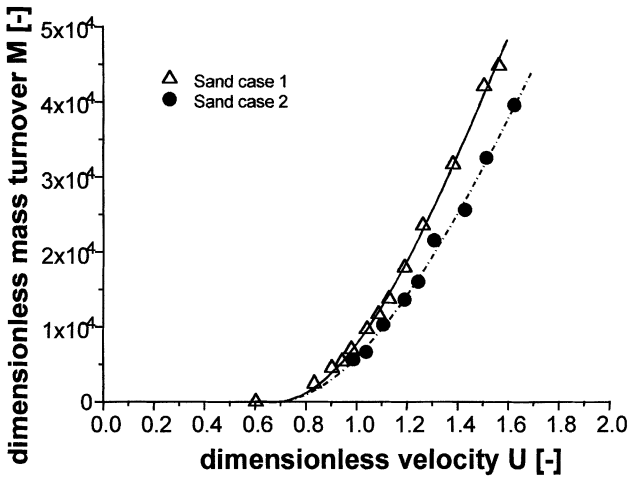

Figure 13. Dimensionless mass turnover of sand for two size distributions.

These experiments confirm that the particle-size distribution is one scaling parameter that should be matched (Glicksman et al., 1994) in order to obtain similarity between a plant and a laboratory model.

Conclusions

From the solid circulation measurements it is concluded that the solid mass turnover defined in Eq. 19 can be used to correlate the behavior in a circulating fluidized bed of particles with a wide range of size and density. It is believed that this parameter is valid not only for the scaled rig used here but also for other types of circulating fluidized beds by suitable adjustment of the fitting parameters a^o. It is also concluded that the solid circulation of a powder is dependent on its particle-size distribution.

For the scale-up of the system discussed here, it is concluded that the fluid-bed gasifier may be scaled according to the rules proposed by Glicksman et al. (1994), since it may be considered to be an ordinary bubbling fluidized bed. On the other hand, the riser should be scaled using the newly introduced scaling parameter for the solid mass turnover, M, rather than the dimensionless solid circulation rate, C_s. The benefit of this procedure is that both particle properties and particle mass load can be varied over a wide range to predict satisfactory values of the solid circulation rate.

Acknowledgment

The authors thank the UCL workshop for building the rig and for constructive discussions during the design phase. The work was carried out under Joule Contract JOR3-CT97-0196, with funds supplied by the European Commission.

Notation

a, b, c, a^*, b^*, c^*, a^o = fitting parameters
A = area, m^2
Ar = Archimedes number [$ar = \rho(\rho_s - \rho)d^3g/\eta^2$]
c = solid volume fraction
c_D = drag coefficient
C_s = dimensionless solid circulation rate ($C_s = G_s/\rho_s u_0$)
D = diameter, m
d = particle diameter, m
$\bar{d}$ = mean particle diameter, m
De = density ratio ($De = \rho_s/\rho$)
d_n = normalized particle diameter
Fr = Froude number ($Fr = u_0^2/Dg$)
g = acceleration due to gravity, m/s^2
GR = geometry ratio ($GR = D/d$)
G_s = mass flux, kg/(m^2·s)
h = height, m
m = total particle-mass load, kg
M = dimensionless mass turnover (defined in Eq. 19)
m^* = mass flow, kg/s
M^o = dimensionless mass load
p' = mean pressure, N/m^2
Re = Reynolds number ($Re = \rho_s u_0 d/\eta$)
t = time, s
u = velocity, m/s
U = ratio of superficial to terminal settling velocity
U^o = ratio of superficial to minimum fluidization velocity
V = volume, m^3
V^* = volumetric flow rate, m^3/s
w, x, y, z = fitting parameters

Greek letters

Δ = difference
ϵ = voidage
η = dynamic viscosity, Pa·s
ϕ = particle-shape factor
ρ = density, kg/m^3

Superscripts and subscripts

0 = superficial
b = bulk
comb = combustor
dc = downcomer
gasi = gasifier
i = interval
mf = minimum fluidization
n = normalized
prim = primary
s = solid
sec = secondary
t = terminal settling

Literature Cited

Almstedt, A. E., and V. Zakkay, "An Investigation of Fluidized-Bed Scaling—Capacitance Probe Measurements in a Pressurized Fluidized-Bed Combustor and a Cold Model Bed," *Chem. Eng. Sci.*, **45**, 1071 (1990).

Caballero, M., M. P. Aznar, J. Gil, J. A. Martin, E. Frances, and J. Corella, "Commercial Steam Reforming Catalysts to Improve Biomass Gasification with Steam-Oxygen Mixtures. 1. Hot Gas Upgrading by the Catalytic Reactor," *Ind. Eng. Chem. Res.*, **36**, 5227 (1997).

Chan, H., and M. Louge, "Fluid Dynamic Similarity of Circulating Fluidized Beds," *Powder Tech.*, **70**, 259 (1992).

Foscolo, P. U., R. Di Felice, L. G. Gibilaro, "Scaling Relationships for Fluidisation: The Generalised Particle Bed Model," *Chem. Eng. Sci.*, **45**, 1647 (1990).

Glicksman, L. R., M. Hyre, and K. Woloshun, "Simplified Scaling Relationships for Fluidized Beds," *Powder Technol.*, **77**, 177 (1993).

Glicksman, L. R., M. R. Hyre, and P. A. Farell, "Dynamic Similarity in Fluidization," *Int. J. Multiphase Flow*, **20**, 331 (1994).

Glicksman, L. R., D. Westphalen, K. Woloshun, "Experimental Scale Models of Circulating Fluidized Bed Combustors," Int. Conf. on Fluidized Bed Combustion, Montreal, Canada (1991).

Horio, M., "Hydrodynamics," *Circulating Fluidized Beds*, J. R. Grace, A. A. Avidan, and T. M. Knowlton, eds., Blackie Academic & Professional, London, p. 21 (1997).

Horio, M., A. Nonaka, Y. Sawa, "A New Similarity Rule for Fluidized Bed Scale-Up," *AIChE J.*, **32**, 1466 (1986).
Molerus, O., *Principles of Flow in Disperse Systems*, Chapman & Hall, London (1993).
Nicastro, N., and L. R. Glicksman, "Experimental Verification of Scaling Relationships for Fluidized Bed," *Chem. Eng. Sci.*, **39**, 1381 (1984).
Nuclear Energy—The Future Climate, The Royal Society, London (1999).
Spliethoff, H., V. Siegel, and K. Hein, *Erforderliche Eigenschaften holz- und halmgutartiger Brennstoffe als Festbrennstoffe bei der Zufeuerung in existierenden Kohlekraftwerken*, Nachwachsende Rohstoffe, Landwirtschaftsverlag GmbH, Münster (1996).
Werther, J., and B. Hirschberg, "Solids Motion and Mixing," *Circulating Fluidized Beds*, J. R. Grace, A. A. Avidan, and T. M. Knowlton, eds., Blackie Academic & Professional, London, p. 119 (1997).
Zhang, M. C., and R. Y. K. Yang, "On the Scaling Laws for Bubbling Gas-Fluidized Bed Dynamics," *Powder Technol.*, **51**, 159 (1987).

Manuscript received Jan. 5, 2000, and revision received Aug. 7, 2000.